How to Choose a Gate Dielectric for Rutile GeO_2

Xiaoru Zhang and Alexander A. Demkov*

Department of Physics, The University of Texas at Austin, Austin, TX 78712, USA

Electrification, renewable-energy conversion, and data-intensive computing require efficient power electronics at high voltage, frequency, and temperature. Wide-bandgap semiconductors address these needs, while ultrawide-bandgap (UWBG) materials offer still larger breakdown fields [1]. Rutile GeO_2 (r-GeO_2) is an emerging UWBG semiconductor with a ≈4.7 eV gap, favorable thermal transport propoerties, predicted possibility of ambipolar doping, and recent demonstration of single-crystal growth and fabrication of MOSFET [2, 3, 4]. However, metal–oxide–semiconductor devices require structurally compatible gate dielectrics with sufficiently large barriers to both electron and hole injection. Because r-GeO_2 has a rather wide gap, satisfying both barrier conditions is especially restrictive [5].

We use first-principles calculations to compare r-GeO_2(001) interfaces with crystalline and amorphous SiO_2, crystalline and amorphous Al_2O_3, and crystalline MgO. Amorphous oxides are generated by melt-and-quench molecular dynamics, and representative atomistic models are shown in Fig. 1. Valence-band offsets are independently determined from core-level alignment, electrostatic-potential lineups, and layer-projected densities of states. The conduction-bnad offsets are then determined using experimental band gap for dielectrics and *ab initio* band gap for r- GeO_2. All five interfaces exhibit type-I band alignment. MgO and Al_2O_3 show asymmetric carrier confinement, with relatively large electron barriers but comparatively weak hole barriers. SiO_2 provides the most balanced confinement for both carrier types.

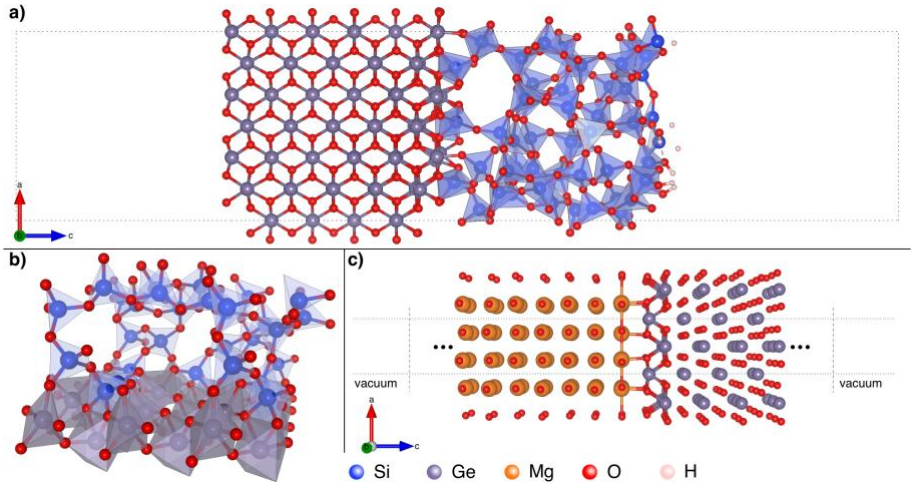

Figure 1. Representative relaxed interface structures. (a) Full amorphous SiO_2/r-GeO_2 slab; the dotted outline marks the supercell. (b) Close-up of the amorphous SiO_2/r-GeO_2 interface. (c) Near-interface region of the crystalline MgO/r-GeO_2 slab.

[1] J. Y. Tsao et al., Adv. Electron. Mater. 4, 1600501 (2018). [2] S. Chae et al., Appl. Phys. Lett. 114, 102104 (2019); [3] P. Emtenani et al., Adv. Funct. Mater. 36, e76723 (2026); [4] K. Tetzner et al., IEEE Electron Device Lett. 47, 566 (2026). [5] J. Robertson, J. Non-Cryst. Solids 303, 94 (2002).

* Author for correspondence: demkov@physics.utexas.edu

Supplementary Information

Interface Construction

Amorphous oxide models. The lateral cell dimensions of the oxide models were matched to the r-GeO_2(001) surface cell. Crystalline SiO_2 and Al_2O_3 precursors were adjusted along the surface normal to reproduce the appropriate mass densities. Amorphous structures were then generated by Born–Oppenheimer molecular dynamics with a Langevin thermostat. Each precursor was melted until representative liquid configurations were obtained, cooled gradually to room temperature, and equilibrated. Diffusive behavior in the liquid was confirmed from the mean-squared displacements, and the quenched structures were validated by comparing their total static structure factors with neutron-scattering data (Fig. S1).

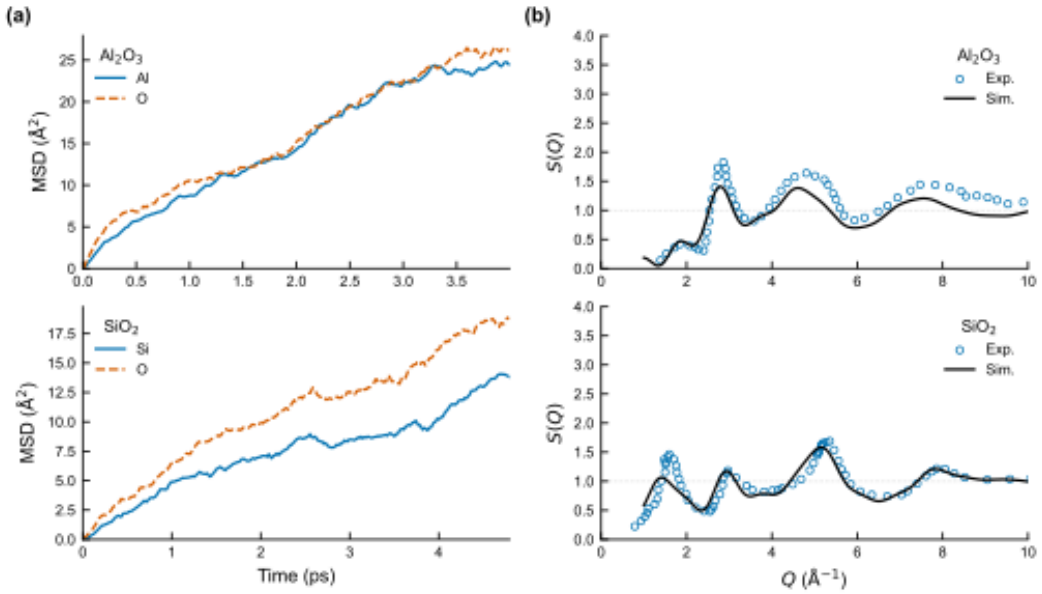

Figure S1. (a) Mean-squared displacements of the constituent species in molten SiO_2 and Al_2O_3. (b) Calculated total static structure factors of the quenched amorphous oxides compared with experimental neutron-scattering data.

Amorphous interfaces. A molten oxide configuration was placed between r-GeO_2(001) substrate regions to form a periodic r-GeO_2–dielectric–r-GeO_2 stack. The dielectric was equilibrated in the molten state while the r-GeO_2 atoms were fixed and was then quenched using the corresponding bulk-oxide protocol. The stack was converted into a slab separated by sufficient vacuum. Undercoordinated atoms at the free SiO_2 surface were H-passivated, whereas the Al_2O_3 surface region was annealed to allow reconstruction. The free r-GeO_2 surface remained unpassivated. All constraints were removed for the final relaxation except where needed to preserve a bulk-like substrate reference region. Several candidates were generated, and a structure with a defect-free, bulk-like dielectric region was retained for each oxide.

Crystalline interfaces. We constructed interfaces with α-cristobalite SiO_2, corundum α-Al_2O_3, and rocksalt MgO. For each oxide, a surface cell was selected and coherently strained in plane to match r-GeO_2(001); the surface-normal lattice vector and all unconstrained internal coordinates were then relaxed. Each slab was separated from its periodic images by sufficient vacuum, and the free crystalline SiO_2 surface was H-passivated.

Band-Alignment Procedure

Definition. The valence-band offset (VBO) is defined as the valence-band maximum (VBM) of r-GeO_2 minus that of the dielectric, so a positive VBO represents a hole barrier that confines holes in r-GeO_2. We determined the VBO with complementary procedures using the same bulk reference calculations and explicit interface models.

Core-level alignment. For each bulk material, we calculated the energy separation between the VBM and a selected core level. The interface calculation then provided the difference between the corresponding core levels in bulk-like regions on the two sides. Combining the two bulk VBM-to-core separations with this interface core-level difference yields the VBO. We used Ge 3p states on the r-GeO_2 side and Si 2p, Al 2p, or Mg 2s states on the dielectric side.

Electrostatic-potential alignment. For each bulk calculation, the VBM was referenced to the local electrostatic potential after planar averaging and subsequent macroscopic averaging. The explicit interface calculation supplied the potential step between the bulk-like r-GeO_2 and dielectric regions. Combining the two bulk VBM-to-potential separations with the interface potential step gives an independent VBO.

Layer-projected density of states. Site-projected densities of states were summed within each atomic layer. The local VBM of a layer was taken as the highest occupied energy for which the integrated filling between mid-gap and the band edge reached the small occupation criterion used in the main text. The VBM was then averaged over the bulk-like layers on each side of the interface, and their difference provided another VBO.

Conduction-band offset. The conduction-band offset (CBO), defined as the dielectric conduction-band minimum minus that of r-GeO_2, was calculated as the dielectric band gap minus the r-GeO_2 band gap minus the VBO. We used a previously calculated ab initio band gap for r-GeO_2 and experimental band gaps for the dielectrics. Thus, the interface-specific lineup comes from the explicit first-principles models, while the CBO is not contaminated by the band-gap underestimation of semilocal DFT.